SISAR: A RIGOROUS ORIENTATION MODEL FOR SYNCHRONOUS AND ASYNCHRONOUS PUSHBROOM SENSORS IMAGERY

M. Crespi[*], F. Fratarcangeli, F. Giannone, F. Pieralice

DITS, Area di Geodesia e Geomatica, Sapienza Università di Roma, via Eudossiana 18, 00184 Rome, Italy
(mattia.crespi, francesca.fratarcangeli, francesca.giannone)@uniroma1.it

Commission I, WG I/5

KEY WORDS: Pushbroom sensors, imagery orientation, rigorous models, software

ABSTRACT:

The correct georeferencing of remote sensing imagery is a fundamental task in the photogrammetric processing for orthoimages, DEM/DSM generation and 3D features extraction. In this paper we focus on the georeferencing of pushbroom sensors imagery with rigorous model, that is the well known approach based on the collinearity equations. In particular, we developed, implemented and tested a rigorous model for the georeferencing both single images and stereopairs collected by EROS A, IKONOS and Quickbird satellites. The model, implemented in the software SISAR, reconstructs the orbital segment during the image acquisition through the Keplerian orbital parameters, and model the sensor attitude and internal orientation allowing for self-calibration parameters too. As regards estimation procedure, in order to avoid instability due to high correlations among some parameters leading to design matrix pseudo-singularity, Singular Value Decomposition (SVD) and QR decomposition are employed to evaluate the actual rank of the design matrix, to select the estimable parameters and finally to solve the linearized collinearity equations system in the least squares sense. The results are compared with rigorous models included in OrthoEngine (PCI Geomatica); three images are concerned in this paper, showing that SISAR performances are at the level of the OrthoEngine ones. In particular, results stemming from the elaborations of Quickbird and IKONOS imagery show that accuracies at sub-meter level, compatible with cartographic product at 1:5000 scale, are achievable. Future prospects regard the rigorous model extension to Cartosat-1, EROS B and Prism satellites.

1. INTRODUCTION

The High Resolution Satellite Imagery (HRSI) have relevant impact for cartographic applications, as possible alternative to aerial photogrammetric imagery to produce maps or orthophotos at 1:5000 scale or lower, for the generation of Digital Elevation Models (DEM) and Digital Surface Models (DSM) and also for 3D feature extraction (e.g. for city modeling), especially in areas where the organization of photogrammetric surveys may result critical.

However, the real possibility of using HRSI for cartography depends on several factors: sensor characteristics (geometric and radiometric resolution and quality), types of products made available by the companies managing the satellites, cost and time needed to obtain these products, cost of suited software for the final processing to realize the cartographic products.

The first and fundamental task to be addressed is the imagery distorsions correction, that is the so called orientation and orthorectification.

The distortions sources can be related to two general categories: the acquisition system, which includes the platform orientation and movement and the imaging sensor optical-geometric characteristics, and the observed object, which takes into account atmosphere refraction and terrain morphology.

At present, HRSI orientation methods can be classified in three categories: black models (like Rational Polynomial Function - RPF), consisting in purely analytic functions linking image to terrain coordinates, independently of specific platform or sensor characteristics and acquisition geometry; physically based models (so called rigorous models), which take into account several aspects influencing the acquisition procedure and are often specialized to each specific platform and sensor; the gray models (like Rational Polynomial Coefficients – RPC models), in which the mentioned RPF are used with known coefficients supplied in the imagery metadata and "blind" produced by companies managing sensors by their own rigorous models.

1.1 SISAR software

Since 2003, the research group at the Area di Geodesia e Geomatica - Sapienza Università di Roma has developed a specific and rigorous model designed for the orientation of imagery acquired by pushbroom sensors carried on satellite platforms, like EROS-A, QuickBird and IKONOS. This model has been implemented in the software SISAR.

The first version of the model (Crespi et al., 2003) was uniquely focused on EROS-A imagery, since no commercial software including a rigorous model for this platform were available at that time. Later, the model was refined (Baiocchi et al., 2004) and extended to process QuickBird Basic imagery too and, at present (since January 2007), the software was extended to IKONOS imagery. The RPC (use and generation) and rigorous orientation of stereo pairs models are now under implementation and the first results are encouraging (Table 1).

2. RIGOROUS MODEL FOR EROS A AND QUICKBIRD SATELLITE

2.1 Model parametrization

The model, implemented in the software SISAR, bases the imagery orientation on the well known collinearity equations, including different subsets of parameters (

Table 2) for the satellite position, the sensor attitude and the viewing geometry (internal orientation and self-calibration).

| SENSOR | SINGLE IMAGE | | STEREO PAIRS |
	Rigorous	RPC (use/generation)	Rigorous
EROS A	YES	YES	YES
QuickBird Basic	YES	YES	YES
IKONOS II	YES	under implementation	under implementation
QuickBird Standard Orthoready	under implementation	under implementation	under implementation

Table 1. SISAR software present facilities

In particular, the satellite position is described through the Keplerian orbital elements attaining to the orbital segment during the image acquisition; the sensor attitude is supposed to be represented by a known time-dependent term plus a 2nd order time-dependent polynomial, one for each attitude angle; moreover, atmospheric refraction is accounted for by a general model for remote sensing applications (Noerdlinger, 1999). The viewing geometry is supposed to be modeled by the focal length and two self-calibration parameters, able to account for a second order distorsion along the array of detectors direction (see Equation (4)).

SATELLITE POSITION	a: semi-major axis e: eccentricity Ω: right ascension of the ascending node i: orbit inclination ω: argument of the perigee v: true anomaly (dependent on T_P, the time of the passage at perigee)
SENSOR ATTITUDE	$\phi=\phi_0(t)+a_0+a_1t+a_2t^2$ (roll) $\theta=\theta_0(t)+b_0+b_1t+b_2t^2$ (pitch) $\psi=\psi_0(t)+c_0+c_1t+c_2t^2$ (yaw)
VIEWING GEOMETRY	f: focal length d_1,d_2: self-calibration parameters

Table 2. Full parametrization of the SISAR model

In order to relate the image to the ground coordinates (expressed in an ECEF reference frame, usually a realization of WGS84, e.g. ITRF2000) by the collinearity equations, a set of rotation matrices (for details see Crespi et al., 2003; Baiocchi et al., 2004; Fratarcangeli F., 2006) involving the following coordinate systems have to be used:

- Image coordinate system (I) - it is a 2D system describing a point position in an image (in pixels); the origin is in the upper left corner, the pixel position is defined by its row (J) and column (I). The column numbers should increase toward the right and row numbers should increase in the downward direction
- Sensor coordinate system (S) - the origin is located at the perspective center (supposed to be coincident with satellite's center of mass), the x_S-axis points to the direction of satellite motion, z_S-axis is directed from the array towards the perspective center, while y_S-axis is parallel to the array of detectors, completing a right-handed system
- Satellite coordinate system (B) - the origin is located at the perspective center (supposed to be coincident with satellite's center of mass) and the x_B, y_B e z_B axes coincide

with the Orbital coordinate system (F) (see below) axes when the attitude angles (ϕ, θ, ψ) are zero. The R_{SB} *(Body-Sensor)* matrix gives the transformation between the B-system and the S-system. It considers the non-parallelism between the axes $(x, y, z)_S$ and $(x, y, z)_B$ and is constant within one scene for each particular sensor; the matrix elements may be provided by metadata files

- Orbital coordinate system (F) - the origin is located at the satellite's center of mass, the x_F-axis is tangent to the orbit directed as the satellite motion, the z_F-axis is in the orbital plane like the x_F-axis and points in the direction of the satellite's center of mass, while y_F-axis completes a right-handed system. The R_{BF} *(Flight-Body)* matrix gives the transformation between the F-system and the B-system through the attitude angles (ϕ, θ, ψ) varying in time; the aforementioned known time-dependent terms (one for each attitude angle: $\phi_0(t)$, $\theta_0(t)$, $\psi_0(t)$) are provided by metadata files

$$R_{BF}=\begin{vmatrix} \cos\psi\cos\vartheta & \sin\psi\cos\varphi+\cos\psi\sin\vartheta\sin\varphi & \sin\psi\sin\varphi-\cos\varphi\cos\psi\sin\vartheta \\ -\cos\vartheta\sin\psi & \cos\psi\cos\varphi-\sin\psi\sin\vartheta\sin\varphi & \cos\psi\sin\varphi+\cos\varphi\sin\psi\sin\vartheta \\ \sin\vartheta & -\cos\vartheta\sin\varphi & \cos\vartheta\cos\varphi \end{vmatrix}$$

(1)

- Earth Centered Inertial (ECI) coordinate system (I) - the origin is located at the Earth's center of mass, the X-axis points to the Vernal Equinox relative to a certain epoch (J2000 -1 January 2000, h 12.00), the Z-axis points to the celestial North Pole in the same epoch while the Y-axis completes a right-handed system. The R_{FI} *(Inertial-Flight)* matrix gives the transformation between the I-system and F-system; it is a function of the Keplerian orbital parameters and thus varies in time within each scene

$$R_{FI}=\begin{vmatrix} -\sin U\cos\Omega-\sin\Omega\cos i\cos U & -\sin\Omega\sin U+\cos U\cos\Omega\cos i & \sin i\cos U \\ -\sin\Omega\sin i & \sin i\cos\Omega & -\cos i \\ \cos\Omega\cos U+\sin\Omega\cos i\sin U & -\sin\Omega\cos U-\cos\Omega\cos i\sin U & -\sin i\sin U \end{vmatrix}$$

(2)

where $U = \omega + v$

Finally, it is well known that the transformation between the considered realization of WGS84 and the ECI coordinate system is driven by precession, nutation, polar motion and Earth rotation matrices (Kaula, 1966).

It is now possible to write the collinearity equations in an explicit form for a generic ground point

$$x_s = f\,\frac{R_1|X_{tI} - X_{SI}|}{R_3|X_{tI} - X_{SI}|} \qquad y_s = f\,\frac{R_2|X_{tI} - X_{SI}|}{R_3|X_{tI} - X_{SI}|} \qquad (3)$$

where (x_s , y_s) are the image coordinates (in metric units), f is the focal length, R_1, R_2, R_3 are the rows of the total rotation matrix $R = R_{SB} R_{BF} R_{FI}$ and (X_{tI} , X_{SI}) are the ground point and the satellite positions in ECI system.

With simple geometric considerations (Figure 1) it is possible to write the collinearity equations as functions of the image coordinates (I , J) (in pixels):

$$\frac{x_s}{f}=tg\beta=\frac{d_{pix}}{f}[J-int(J)-J_0]$$

$$\frac{y_s}{f}=-tg\alpha=-\frac{d_{pix}}{f}[d_1(I-I_0)+d_2(I-I_0)^2]$$

(4)

where d_{pix} is the image pixel dimension and (I_0 , J_0) are the principal point coordinates (in pixels). It has to be noted that J_0 may be assumed equal to 0.5 and two self-calibration parameters are included in the second equation (4) only; on the contrary, it is not introduced a third self-calibration parameter K suited to account for a possible misalignment of the pixel array in the focal plane, affecting the J coordinate, since it is not estimable separately from the sensor attitude parameters.

Substituting equations (4) into equations (3) the collinearity equations become:

$$R_1|X_{tI} - X_{SI}| - \left(\frac{d_{pix}}{f}[J - \text{int}(J) - J_0]\right)R_3|X_{tI} - X_{SI}| = 0$$

$$R_2|X_{tI} - X_{SI}| + \left(\frac{d_{pix}}{f}[d_1(I - I_0) + d_2(I - I_0)^2]\right)R_3|X_{tI} - X_{SI}| = 0 \qquad (5)$$

these equations are linearized with respect to both the parameters aforementioned and to the image and ground coordinates (Teunissen, 2001).
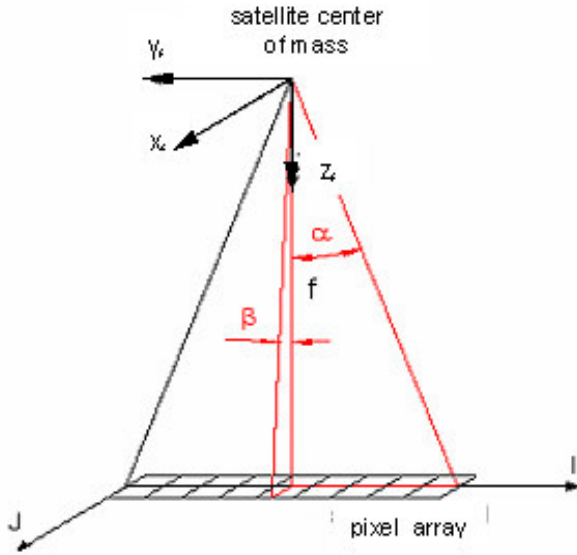

Figure 1. Sensor (S) and Image (I) coordinate systems

2.2 Parameter estimation strategy

As regards the full parametrization aforementioned, two major items have to be underlined:

- approximate values for all parameters may be derived from the information contained into the metadata files released together with the imagery or they are simply fixed to zero (2nd order polynomial coefficients for attitude angles); nevertheless, it has to be noted that EROS A metadata are quite scarce (few state vectors for positions and attitudes along the orbital arc) and may be quite rough (errors up to kilometers for the imagery direct georeferencing) so that a preliminar improvement is generally useful, whilst QuickBird metadata are quite rich (hundreds of state vectors for positions and attitudes along the orbital arc) and accurate (errors within few tens of meters for the imagery direct georeferencing)
- in theory, these approximate values must be corrected by an estimation process based on a suitable number of Ground Control Points (GCPs), for which collinearity

equations are written; nevertheless, since the orbital arc related to each image acquisition is extremely short (few hundreds of kilometers) if compared to the whole orbit lenght (some thousandths), some Keplerian parameters are not estimable at all (a, e, ω) and others (i, Ω, T_P) are extremely correlated among them and with sensor attitude and viewing geometry parameters

In order to avoid instability due to high correlations among some parameters leading to design matrix pseudo-singularity, Singular Value Decomposition (SVD) and QR decomposition are employed to evaluate the actual rank of the design matrix, to select the estimable parameters and finally to solve the linearized collinearity equations system in the least squares (LS) sense.

In details, at first it is necessary to select the parameters estimable from the observations for the system of linear equations (Ax=b), with $A \in \Re^{mxn}$ (m≥n); the remaining parameters need to be constrained to their initial (approximate) values. We adopt an SVD-based subset selection procedure due to Golub, Klema and Stewart (Golub et al., 1993; Strang et al., 1997) that proceeds as follows:

1. The SVD $A = UWV^T$ is computed and used to determine the actual rank r of the design matrix A; the threshold used to evaluate r is based on the ratio between the maximum and the allowed minimum singular values; reference values are $10^{-4} \div 10^{-5}$ (for further details see (Press et al., 1992))

2. An independent subset of r columns of A is selected by the QR decomposition QR=AP. In a system of linear equations (Ax=b), if A has a rank r, the QR decomposition produces the factorization AP=QR where R is:

$$R = Q^T AP = \begin{bmatrix} R_{11} & R_{12} \\ 0 & 0 \end{bmatrix} \begin{matrix} \to r \\ \to m-r \end{matrix}$$
$$\begin{matrix} \downarrow & \downarrow \\ r & n-r \end{matrix}$$

As for the LS problem the quadratic form:

$$\|Ax - b\|_2^2 = \|(Q^T AP)(P^T x) - Q^T b\|_2^2 = \|R_{11}y - (c - R_{12}z)\|_2^2 + \|d\|_2^2$$

is considered, where

$$P^T x = \begin{bmatrix} y \\ z \end{bmatrix} \begin{matrix} \to r \\ \to n-r \end{matrix} \quad \text{and} \quad Q^T b = \begin{bmatrix} c \\ d \end{bmatrix} \begin{matrix} \to r \\ \to m-r \end{matrix}$$

if x is a LS minimizer we obtain:

$$x = P \begin{bmatrix} R_{11}^{-1}(c - R_{12}z) \\ z \end{bmatrix}$$

Therefore, if z is a set of zeroes in this expression, we can derive the basic solution $x_B \in \Re^r$ from:

$$x_B = P \begin{bmatrix} R_{11}^{-1}c \\ 0 \end{bmatrix} \quad \text{and} \quad R_{11}x_B = Q^T b$$

Then, if we set:

$$y = P\begin{bmatrix} x_B \\ 0 \end{bmatrix} \qquad (6)$$

Ay is a LS predictor of b that involves the first r columns of AP.

The permutation matrix P is calculated so that the columns of the matrix $B_1 \in \Re^{mxn}$ in AP=[B_1 B_2] are "sufficiently independent"

3. Finally, b is predicted with the vector Ay where y is described in the equation (6), and z minimizes $\|B_1 x_B - b\|_2$

Moreover, the statistical significance of each estimable parameters is checked by a Student T-test so to avoid overparametrization; in case of not statistically significant parameter, it is removed and the estimation process is repeated until all parameters are significant.

As usual, the solution related to the estimable parameters only is obtained iteratively due to non linearity; the iterative procedure is stopped when the estimated variance of unit weight $\hat{\sigma}_0$ reaches a minimum. Before the second iteration, it is evaluated the ground displacement due to atmospheric refraction at each GCP; GCP coordinates are corrected in order to eliminate the refraction effect, which is relevant under large *off-nadir* acquisition angles (less than 0.5 m at 10°, 2 m at 30°, more than 7 m at 50°).

The formal structure of the functional model with full parametrization for the final estimation is the following

$$A\xi + D\eta + d = 0 \qquad (6)$$

where A is the design matrix

$$A = \begin{vmatrix} A_1 \\ A_2 \\ . \\ A_n \end{vmatrix} \quad A_i = \begin{vmatrix} \frac{\partial F_1}{\partial a_0} & \frac{\partial F_1}{\partial a_1} & \frac{\partial F_1}{\partial a_2} & \frac{\partial F_1}{\partial b_0} & \frac{\partial F_1}{\partial b_1} & \frac{\partial F_1}{\partial b_2} & \frac{\partial F_1}{\partial c_0} & \frac{\partial F_1}{\partial c_1} & \frac{\partial F_1}{\partial c_2} & \frac{\partial F_1}{\partial f} & \frac{\partial F_1}{\partial T_p} & \frac{\partial F_1}{\partial d_1} & \frac{\partial F_1}{\partial d_2} \\ \frac{\partial F_2}{\partial a_0} & \frac{\partial F_2}{\partial a_1} & \frac{\partial F_2}{\partial a_2} & \frac{\partial F_2}{\partial b_0} & \frac{\partial F_2}{\partial b_1} & \frac{\partial F_2}{\partial b_2} & \frac{\partial F_2}{\partial c_0} & \frac{\partial F_2}{\partial c_1} & \frac{\partial F_2}{\partial c_2} & \frac{\partial F_2}{\partial f} & \frac{\partial F_2}{\partial T_p} & \frac{\partial F_2}{\partial d_1} & \frac{\partial F_2}{\partial d_2} \end{vmatrix}$$
$$(7)$$

D is the matrix of observation coefficients

$$D = \begin{vmatrix} D_1 & & & \emptyset \\ & D_2 & & \\ & & . & \\ \emptyset & & & D_n \end{vmatrix} \quad D_i = \begin{vmatrix} \frac{\partial F_1}{\partial I} & \frac{\partial F_1}{\partial J} & \frac{\partial F_1}{\partial X_t} & \frac{\partial F_1}{\partial Y_t} & \frac{\partial F_1}{\partial Z_t} \\ \frac{\partial F_2}{\partial I} & \frac{\partial F_2}{\partial J} & \frac{\partial F_1}{\partial X_t} & \frac{\partial F_1}{\partial Y_t} & \frac{\partial F_1}{\partial Z_t} \end{vmatrix} \quad (8)$$

d is the known term

$$d = \begin{vmatrix} d_1 \\ . \\ . \\ d_n \end{vmatrix} \quad d_i = \begin{vmatrix} F_1(\tilde{y}, \tilde{x}) \\ F_2(\tilde{y}, \tilde{x}) \end{vmatrix} \quad (9)$$

ξ, η are respectively the parameters (corrections to their approximate values) and the corrections to the observations (image and GCP coordinates).

As regards the stochastic model, a simple diagonal cofactor matrix for observation (I, J; X_t, Y_t, Z_t) is assumed; standard deviations of the image observations are set equal considering that manual collimation tests carried out independently by different operators showed that an accuracy ranging from 1/3 to 1/2 pixel in image coordinates may be routinely achieved; for the GCP coordinates standard deviations are usually set equal to mean values obtained during their direct surveys or cartographic selection.

At the end of the estimation process, the achievable external accuracy is evaluated by the RMSE of the Check Points (CPs) coordinate residuals; it is well known that CPs are known ground points not used in the parameter estimation process. It has to be underlined that the atmospheric refraction is accounted for in this case too.

3. RIGOROUS MODEL FOR IKONOS SATELLITE

Recently, the SISAR software was extended to process the IKONOS Geo Ortho Kit type imagery.

This kind of imagery are completely different with respect to EROS A and QuickBird Basic ones because they are pre-processed (1B level): they are map projected to a datum (ellipsoid at the mean elevation of the covered area) and map projection system; they also undergo a correction process to remove image distortions and to resample it to a uniform Ground Sampling Distance (GSD).

The rigorous model implemented in the SISAR software is always based on collinearity equations, which, in this case, may be directly written in ECEF coordinates:

$$\begin{vmatrix} X_I - X_S \\ Y_I - Y_S \\ Z_I - Z_S \end{vmatrix} = \lambda R \begin{vmatrix} X_T - X_S \\ Y_T - Y_S \\ Z_T - Z_S \end{vmatrix} \Rightarrow \begin{cases} \dfrac{X_I - X_S}{Z_I - Z_S} = \dfrac{R_1|X_T - X_S|}{R_3|Z_T - Z_S|} \\ \dfrac{Y_I - Y_S}{Z_I - Z_S} = \dfrac{R_2|Y_T - Y_S|}{R_3|Z_T - Z_S|} \end{cases} \quad (10)$$

where (X_I, Y_I, Z_I) are the image coordinates, (X_S, Y_S, Z_S) the (approximate) satellite coordinates and (X_T, Y_T, Z_T) the ground coordinates in ECEF, λ is a scale factor and R_1, R_2, R_3 are the rows of a rotation matrix.

The (X_I, Y_I, Z_I) coordinates are computed from the coordinates (in pixels) in the Image system (I, J) and the information available in the metadata file:

$$\begin{cases} N_I = N_A - J \cdot p \\ E_I = E_A + I \cdot p \end{cases}$$

where (N_A, E_A) are the upper left corner coordinates of the image (available on metadata file), p is the GSD (available on metadata file)

The initial (X_S, Y_S, Z_S) coordinates are simply computed starting from the Nominal Collection Elevation and the Nominal Collection Azimuth available in the metadata file (Figure 2).
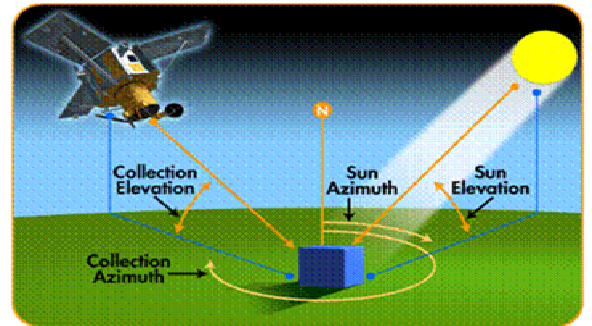

Figure 2. Information about IKONOS acquisition
(Courtesy of Dr. Tine Flingelli – European Space Imaging)

Moreover, satellite position is computed for each acquired image line accounting for approximate information about

IKONOS orbit (always descendent, with an inclination angle of about 98.2°) and acquisition mode (Forward or Reverse Scan and Scan Azimut), these last data being included into the metadata file. Since the direct georeferencing is at the level of tens of meters, the rotation matrix can be linearized in the following way:

$$R = I + \delta R = \begin{vmatrix} 1 & a & b \\ -a & 1 & c \\ -b & -c & 1 \end{vmatrix}$$

where three parameters (*a, b, c*) are considered time-dependent at the first or second order. Therefore, the collinearity equations (10) contain 6 (linear dependency) or 9 (quadratic dependency) parameters, which have to be estimated in least squares sense. The statistical significance of the parameters are checked by a Student T-test so to avoid overparametrization as before.

4. RESULTS

The results of rigorous models implemented in SISAR have been analyzed and compared with the ones obtained by the rigorous models developed by Thierry Toutin (Toutin, 2004), implemented in the software OrthoEngine (PCI Geomatica) v. 10.0.

The models were compared on several images; in this context we only analyze the results attaining to three image with different features (Table 3). For each image and for each software the images were oriented varying the GCPs number and analyzing the overall accuracy (RMSE of CP residuals) both for North and East coordinates. In all cases ground points (used both as GCPs and CPs) were collected by RTK or fast-static surveys with GPS receivers of geodetic class, so that their mean accuracy (1 sigma) is around 5-10 cm horizontally and 10-20 cm in the height.

SENSOR	GSD [m]	OFF-NADIR ANGLE (°)		SCENE COVERAGE (Km*Km)	GCP
		START	END		
EROS A	2.60	**31.0**	**40.1**	17x12	49
QuickBird	0.67	20.0		**48x19**	57
IKONOS	1.00	18.7		11x10	27

Table 3. Test images

4.1 EROS A

This image collected over Rome is particular because exhibits a remarkable mean off-nadir angle.
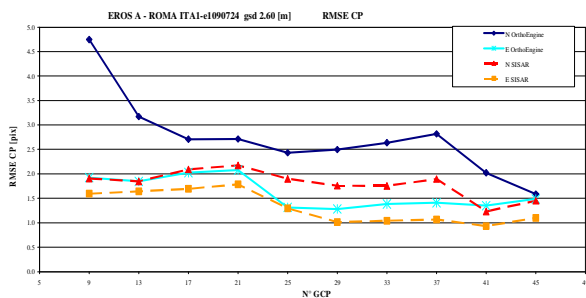

Figure 3. Accuracy vs. GCPs number for EROS image

Both software reach the accuracy assessment with 25-29 GCPs, but SISAR seems perform better especially with few GCPs. Accuracies are respectively at the level of 1.8 (North) and 1.1 (East) pixel for SISAR and at the level of 2.5 (North) and 1.3 (East) pixel for OrthoEngine (Figure 3).

Shortly recalling the results obtained with other EROS A imagery, overall SISAR seems perform better than OrthoEngine with more inclined (higher off-nadir angle) images and vice versa.

4.2 QuickBird

The Salerno image was created joining three different QuickBird images coming from the same orbital passage. The particularity of this image is its latitude extension, about 48 Km. Both software reach the accuracy assessment with 25-29 GCPs; SISAR seem perform better than Orthoengine for East component (0.6 vs. 1.0 pixels) whilst the behaviour is similar for North component (1.2 pixels) (Figure 4).
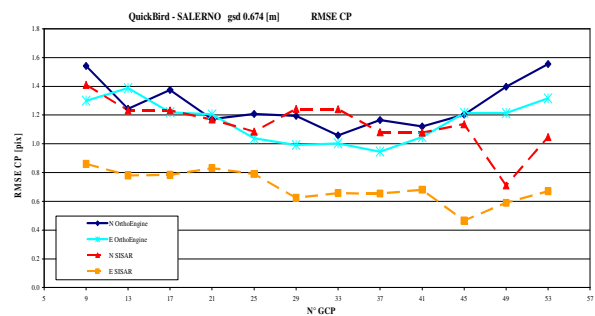

Figure 4. Accuracy vs. GCPs number for Quickbird image

Shortly recalling the results obtained with other Quickbird imagery, overall SISAR and OrthoEngine exhibit similar performances.

4.3 IKONOS II

The Rome image is quite standard as regards off-nadir angle and dimension.

Both software reach the accuracy assessment with 15-20 GCPs and performances are similar (slightly better SISAR for the East component, vice versa for the North one) (Figure 5).
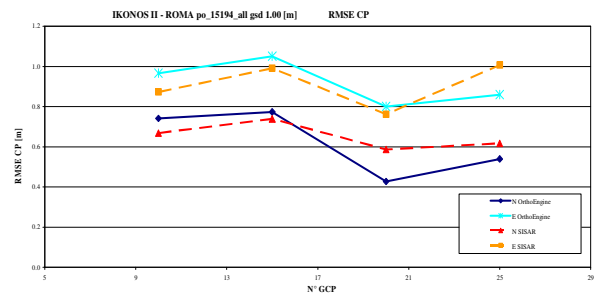

Figure 5. Accuracy vs. GCPs number for IKONOS image

5. CONCLUSIONS

Original rigorous models for the orientation of basic imagery (level 1A) collected by EROS A and QuickBird and pre-processed IKONOS Geo Ortho Kit imagery (level 1B) were

developed and implemented into the software SISAR at the Area di Geodesia e Geomatica - Sapienza Università di Roma.

A particular care was devoted to the analysis of parameters estimability, selection and significance, what appear a quite new topic in the frame of rigorous model for HRSI orientation. In this respect, an automatic parameter selection strategy based on the Singular Value Decomposition (SVD) followed by a QR decomposition applied to the design matrix were implemented.

To point out the effectiveness of the new models, SISAR results were compared with the corresponding ones obtained by the well known software OrthoEngine (PCI Geomatica) v. 10.0, where Thierry Toutin's rigorous models for the imagery orientation of the main HRSI are implemented. In details, three images were concerned, showing that SISAR performances are at the level of the OrthoEngine ones. In particular, results stemming from the elaborations of Quickbird and IKONOS imagery show that accuracies at sub-meter level, compatible with cartographic product at 1:5000 scale, are achievable.

A more complete comparison, also including tests on stereo pairs and concerning other well known software (ERDAS, ENVI), with a more detailed illustration of the SISAR models, will be discussed into a paper presently under preparation.

Future prospects regard the rigorous model extension to Cartosat-1, EROS B and Prism satellites.

ACKNOWLEDGMENTS

REFERENCES

Baiocchi V., Crespi M., De Vendictis L., Giannone F., 2004. A new rigorous model for the orthorectification of synchronous and asynchronous high resolution imagery. Proc. of the 24th EARSeL Symposium, Dubrovnik (Croatia), pp. 461-468

Crespi M., Baiocchi V., De Vendictis L., Lorenzon F., Mezzapesa M. & Tius E., 2003. A new method to orthorectify EROS A1 imagery. Proc. of 2003 Tyrrhenian International Workshop on Remote Sensing, pp. 566-575

Fratarcangeli F., 2006. Ortorettificazione di immagini satellitari ad alta risoluzione acquisite dalla piattaforma QuickBird: sviluppo di un modello rigoroso ed implementazione di un software. Degree thesis in Environmental Engineering (in Italian), Area di Geodesia e Geomatica Dipartimento di Idraulica Trasporti e Strade, Sapienza Università di Roma.

Giannone F., 2006. A rigorous model for High Resolution Satellite Imagery Orientation. PhD Thesis, Area di Geodesia e Geomatica Dipartimento di Idraulica Trasporti e Strade, Sapienza Università di Roma.

Golub G. H., Van Loan C. F., 1993. *Matrix Computation*. The Johns Hopkins University Press, Baltimore and London.

Kaula W. M., 1966. *Theory of Satellite Geodesy*. Blaisdell Publishing Company.

Noerdlinger P. D., 1999. Atmospheric refraction effects in Earth remote sensing. *ISPRS Journal of Photogrammetry & Remote Sensing*, 54, pp. 360–373.

Press W. H., Teukolsky S. A., Vetterling W. T., Flannery B. P., 1992. *Numerical Recipes in C: The Art of Scientific Computing*. Cambridge University Press (ISBN 0-521-43108-5), http://www.nr.com (accessed on April 10, 2006).

Strang G., Borre K., 1997. *Linear Algebra, Geodesy and GPS*. Wellesley-Cambridge Press, Wellesley.

Teunissen P. J. G., 2001. *Adjustment theory. Series on Mathematical Geodesy and Positioning*. Delft University Press

Toutin T., 2004. Review article: Geometric processing of remote sensing images: models, algorithms and methods, *International Journal of Remote Sensing*, 25, pp. 1893-1924.